Available online at www.sciencedirect.com
ScienceDirect
Journal of Solid State Chemistry 181 (2008) 221–227
JOURNAL OF SOLID STATE CHEMISTRY
www.elsevier.com/locate/jssc

Two new hydrogen bond-supported supramolecular compounds assembly from arsenic vanadates and $[M(H_2O)_6]^{2+}$ cations (M = Co, Ni)

Xiao-Bing Cui[a], Ke-Chang Li[a], Ling Ye[b], Yan Chen[a], Ji-Qing Xu[a,*], Wei-Jie Duan[a], Hai-Hui Yu[a], Zhi-Hui Yi[a], Ji-Wen Cui[a]

[a]*State Key Laboratory of Inorganic Synthesis and Preparative Chemistry, College of Chemistry, Jilin University, Changchun 130023, China*
[b]*Key Laboratory of Supramolecular Structure and Materials of Ministry of Education, Jilin University, Changchun 130023, China*

Received 6 June 2007; received in revised form 15 November 2007; accepted 19 November 2007

Abstract

Two new supramolecular compounds based on arsenic vanadates formulated as $[H_2As_6V_{15}O_{42}(H_2O)][Co(H_2O)_6]_2 \cdot 2H_2O$ (**1**) and $[H_2As_6V_{15}O_{42}(H_2O)][Ni(H_2O)_6]_2 \cdot 2H_2O$ (**2**) have been prepared by reacting V_2O_5, $H_2C_2O_4 \cdot 2H_2O$, As_2O_3, $\cdot H_2SO_4$, $CoCl_2 \cdot 6H_2O$ ($NiSO_4 \cdot 6H_2O$) and enMe (enMe = 1,2-diaminopropane) under mild hydrothermal conditions and characterized by elemental analyses, IR, ESR, XPS and single crystal X-ray diffraction analyses. Crystal structure analyses reveal that compounds **1** and **2** are isostructural and exhibit novel 2-D supramolecular layer structures constructed from arsenic–vanadium clusters and two different types of secondary building units (SBUs), respectively, the different SBUs are formed by joint of two adjacent $[Co(H_2O)_6]^{2+}$ cations in compounds **1** and $[Ni(H_2O)_6]^{2+}$ cations in **2**, respectively.

Keywords: Supramolecular; Hydrothermal; Polyoxometalate; Hydrogen bond; Crystal structure

1. Introduction

In the past 30 years, supramolecular chemistry has developed at a tremendous rate. This expansion has been driven by the growing knowledge regarding synthetic and characterization methods for complex structures [1–3]. The directed assembly of supramolecular arrays from discrete molecular building blocks is a topic of significant interest with potential applications in the areas of catalysis, molecular electronics, sensor design, and optics [4–9]. In the construction of supramolecular materials, one important strategy is that those of low-dimensional building blocks extend to high-dimensional networks through weak intermolecular interactions, including hydrogen-bonding, $\pi\cdots\pi$ stacking and weak van der Waals interactions, etc. Doubtless, the hydrogen bond is the most familiar organizing force in supramolecular assembles by virtue of its unique strength and directionality that may control short-range packing [10].

Supramolecular compounds based on polyoxometalates (POMs) have been unexplored in past decades, though the spherical surface of the POMs gives a better opportunity in forming hydrogen bonds with the organic/inorganic moieties. In recent years, extensive efforts have been focused on the design and assembly of such kind of supramolecular architectures and a few high-dimensional supramolecular architectures have been synthesized [11–13].

A prominent subclass of POMs is the family of arsenic–vanadium clusters with arsenic and vanadium in low oxidation states, which generally can be divided into two distinct types based on the numbers of the arsenic and vanadium atoms: As_8V_{14} and As_6V_{15} clusters. The first case is represented by anions $[As_8V_{14}O_{42}(X)]^{6-}$ ($X = SO_3^{2-}$ or SO_4^{2-}) [14] and compound $[N(Me)_4]_4[As_8V_{14}O_{42}(H_2O)_{0.5}]$, [15] while the second group is exemplified by compounds

*Corresponding author.
E-mail addresses: cuixb@mail.jlu.edu.cn (X.-B. Cui), xjq@mail.jlu.edu.cn (J.-Q. Xu).

0022-4596/$ - see front matter © 2007 Elsevier Inc. All rights reserved.
doi:10.1016/j.jssc.2007.11.020

$K_6[As_6V_{15}O_{42}(H_2O)]\cdot 8H_2O$ [16] and $K_6[As_6V_{15}O_{42}(H_2O)]\cdot 6H_2O$ [17].

As a continuous effort to the class of arsenic–vanadium cluster [18,19], we recently have focused on the use of As–V clusters as structural building blocks in the syntheses of hydrogen-bonded high-dimensional structures, for hydrogen-bonded high-dimensional assembly of arsenic–vanadium system has not been explored thoroughly. In this paper, we report two supramolecular assemblies: $[H_2As_6V_{15}O_{42}(H_2O)][Co(H_2O)_6]_2\cdot 2H_2O$ (**1**) and $[H_2As_6V_{15}O_{42}(H_2O)][Ni(H_2O)_6]_2\cdot 2H_2O$ (**2**), which are isostructural and exhibit novel supramolecular arrays based on arsenic-vanadium clusters.

2. Experimental

2.1. General procedures

All chemicals purchased were of reagent grade and used without further purification. Inductively coupled plasma (ICP) analyses were conducted on a Perkin-Elmer Optima 3300 DV spectrometer. Determination of electron spin resonance (ESR) was carried out on Bruker ER 200D-SRC spectrometer. Infrared spectra were recorded as KBr pellets on a Perkin-Elmer SPECTRUM ONE FTIR spectrophotometer. XPS analysis was performed on a VG ESCALAB MKII spectrometer with a Mg $K\alpha$ (1253.6 eV) achromatic X-ray source. Temperature-dependent magnetic susceptibility data for polycrystalline compounds **1**, **2** were recorded on a Quantum Design MPMS XL-5 SQUID magnetometer under an applied field of 1000 Oe over the temperature range in 4–300 K.

2.2. Synthesis

2.2.1. Synthesis of $[H_2As_6V_{15}O_{42}(H_2O)][Co(H_2O)_6]_2\cdot 2H_2O$ (*1*)

A mixture of V_2O_5 (0.36 g, 2.0 mmol), $H_2C_2O_4\cdot 2H_2O$ (0.25 g, 2.0 mmol), As_2O_3 (0.20 g, 1.0 mmol), H_2SO_4 (1 mol L^{-1}, 2 ml, 2.0 mmol), $CoCl_2\cdot 6H_2O$ (0.24 g, 1.0 mmol), enMe (enMe = 1,2-diaminopropane, 0.17 mL, 2.0 mmol) and H_2O (8 mL, 444 mmol) in a molar ratio of 2:2:1:2:1:2:444 was stirred for 30 min, then $NH_3\cdot H_2O$ was added to adjust the pH value to 10, finally the suspension was transferred to a 15 ml Telfon-lined stainless steal autoclave and heated at 160 °C for 3 days. After cooling to room temperature, black block crystals were isolated, washed with water, and dried at room temperature (yield: 75% based on V). IR (KBr pellets cm^{-1}): 3337 s, 1610 m, 1404 m, 1224 m, 985 vs, 727 vs, 632 s, 463 m. Calcd. for H5.33AsCo0.33O9.5V2.5: As, 19.75; Co, 5.13; V, 33.58%. Found: As, 19.63; Co, 4.97; V, 33.51%.

2.2.2. Synthesis of $[H_2As_6V_{15}O_{42}(H_2O)][Ni(H_2O)_6]_2\cdot 2H_2O$ (*2*)

The same procedure as that for **1** was followed, except for using 0.26 g of $NiSO_4\cdot 6H_2O$. Yield is 53% based on V. IR data for **2** in cm^{-1}: 3343 s, 1626 m, 1232 s, 989 vs, 727 vs, 630 s, 464 m. Anal. Calcd. for H5.33AsNi0.33O9.5V2.5: As, 19.77; Ni, 5.11; V, 33.60%. Found: As, 19.67; Ni, 5.03; V, 33.45%.

Table 1
Crystal data and structure refinement parameters for **1** and **2**

Empirical formula	$H_{5.33}AsCo_{0.33}O_{9.5}V_{2.5}$	$H_{5.33}AsNi_{0.33}O_{9.5}V_{2.5}$
Formula weight	379.29	379.21
Crystal system	Hexagonal	Hexagonal
Space group	*P*6322	*P*6322
a (Å)	12.5402(18)	12.5269(18)
b (Å)	12.5402(18)	12.5269(18)
c (Å)	23.863(5)	23.884(5)
α (°)	90	90
β (°)	90	90
γ (°)	120	120
V (Å^3)	3249.9(9)	3245.8(9)
Z	12	12
D_c (g cm^{-3})	2.326	2.328
μ (mm^{-1})	5.675	5.751
$F(0\,0\,0)$	2170	2174
Crystal size (mm)	$0.36\times0.32\times0.26$	$0.40\times0.39\times0.22$
θ ranges (°)	3.17–27.48.	3.17–27.46
Reflections collected	31781	31597
R_{int} value	0.069767	0.061223
Completeness to θ	99.7%	99.7 %
Goodness-of-fit on F^2	1.094	1.069
Final R indices	$R_1 = 0.0356$,	$R_1 = 0.0427$,
$[I>2\sigma(I)]$	$wR_2 = 0.1133$	$wR_2 = 0.1377$
R indices (all data)	$R_1 = 0.0394$,	$R_1 = 0.0463$,
	$wR_2 = 0.1155$	$wR_2 = 0.1406$
Abs-structure-flack	0.00	0.00

$R_1 = \Sigma||F_0|-|F_c||/\Sigma|F_0|$; $wR_2 = [\Sigma w(F_0^2 - F_c^2)^2/\Sigma w(F_0^2)^2]^{1/2}$.

2.3. X-ray crystallography

The reflection intensity data for **1** and **2** were measured at 293 K on a Rigaku R-AXIS RAPID IP diffractometer with graphite monochromated Mo $K\alpha$ ($\lambda = 0.71073$ Å) radiation. Neither of the crystals showed evidence of crystal decay during data collection. Both structures were solved by direct methods and refined using the full-matrix least squares on F2 with SHELXTL-97 crystallographic software package. In the final refinements, all atoms were refined anisotropically, while no H atoms were included in the models. It should be noted that in each compound disorder is observed for the lattice water, O4W for compound **1** is disordered over three positions with occupancies of 1/3 respectively, while O4W for compound **2** shows the same disordered characteristic. A summary of the crystallographic data and structure refinements for compounds **1** and **2** are given in Table 1. Selected bond lengths of compounds **1** and **2** are listed in Table 2.

3. Result and discussion

3.1. Synthesis

The supramolecular compounds of this study were prepared by conventional hydrothermal methods [20,21],

Table 2
Selected bond lengths for compounds **1** and **2**

Compound **1**		Compound **2**	
As(1)–O(4)	1.769(4)	As(1)–O(5)	1.766(5)
As(1)–O(3)	1.775(4)	As(1)–O(7)	1.771(5)
As(1)–O(8)	1.789(2)	As(1)–O(2)	1.784(3)
V(1)–O(2)	1.610(4)	V(1)–O(4)	1.590(6)
V(1)–O(6)	1.920(4)	V(1)–O(1)#5	1.931(4)
V(1)–O(7)	1.936(4)	V(1)–O(1)#7	1.931(4)
V(1)–O(3)	1.981(4)	V(1)–O(5)	1.987(5)
V(1)–O(4)#1	1.990(4)	V(1)–O(5)#4	1.987(5)
V(2)–O(1)	1.610(4)	V(2)–O(8)	1.612(5)
V(2)–O(6)	1.931(4)	V(2)–O(3)	1.930(5)
V(2)–O(6)#3	1.939(4)	V(2)–O(1)#5	1.934(4)
V(2)–O(7)#3	1.946(4)	V(2)–O(3)#5	1.936(5)
V(2)–O(3)	2.031(4)	V(2)–O(7)	2.032(5)
V(3)–O(5)	1.581(5)	V(3)–O(6)	1.613(5)
V(3)–O(7)#1	1.926(4)	V(3)–O(3)	1.919(5)
V(3)–O(7)#3	1.926(4)	V(3)–O(1)	1.935(5)
V(3)–O(4)#4	1.992(4)	V(3)–O(7)	1.981(5)
V(3)–O(4)	1.992(4)	V(3)–O(5)#7	1.987(4)
O(4)–V(1)#1	1.990(4)	Ni(1)–O(1W)#2	2.147(6)
O(6)–V(2)#2	1.939(4)	Ni(1)–O(1W)#3	2.147(6)
O(7)–V(3)#2	1.926(4)	Ni(1)–O(1W)	2.147(6)
O(7)–V(2)#2	1.946(4)	Ni(1)–O(2W)#2	2.171(6)
O(8)–As(1)#1	1.789(2)	Ni(1)–O(2W)	2.171(6)
Co(1)–O(1W)#5	2.195(5)	Ni(1)–O(2W)#3	2.171(6)
Co(1)–O(1W)	2.195(5)	O(1)–V(1)#6	1.931(4)
Co(1)–O(1W)#6	2.195(5)	O(1)–V(2)#6	1.934(4)
Co(1)–O(2W)#6	2.196(5)	O(2)–As(1)#7	1.784(3)
Co(1)–O(2W)	2.196(5)	O(3)–V(2)#6	1.936(5)
Co(1)–O(2W)#5	2.196(5)	O(5)–V(3)#7	1.987(4)

Symmetry transformations used to generate equivalent atoms: (#1) $-x+y$, y, $-z+1/2$; (#2) $-x+y$, $-x+1$, z; (#3) $-y+1$, $x-y+1$, z; (#4) $-y+1$, $-x+1$, $-z+1/2$; (#5) $-x+y+1$, $-x+1$, z; (#6) $-y+1$, $x-y$, z; and (#7) x, $x-y$, $-z+1/2$.

which are now routinely applied to the isolation of POM compounds [22]. The compounds **1** and **2** were prepared by adjustments of the pH of the mixture of V_2O_5, $H_2C_2O_4\cdot 2H_2O$, As_2O_3, H_2SO_4, $CoCl_2\cdot 6H_2O$ or $NiSO_4\cdot 6H_2O$, enMe and H_2O to 10.0 through the addition of an amount of $NH_3\cdot H_2O$. If $NH_3\cdot H_2O$ was replaced by solution of KOH or NaOH, only microcrystalline materials could be isolated. $NH_3\cdot H_2O$ presumably modifies the solubility of the reactants and products and promotes crystal growth. The pH value of reaction systems is a crucial factor effecting formation of the products, if the reactions were carried out at lower pH (<10), no crystals were formed. $H_2C_2O_4\cdot 2H_2O$ and enMe provide the reductants for vanadium. The enMe is also an important factor for the formation of the two compounds, if we did not added enMe, only undetermined powders were got. If we did not added $H_2C_2O_4\cdot 2H_2O$ in the reaction systems, we get lower yield. We also tried the reactions without the addition of the H_2SO_4 solution, getting the two compounds with lower yield too.

3.2. Structure descriptions

Single-crystal X-ray diffraction and elemental analyses performed on the complexes **1** and **2** reveal that they are isostructural with slight differences in bond lengths and angles. Here complex **1** is taken as an example to present and discuss the structure in detail.

3.2.1. Crystal structure of *1*

The arsenic–vanadium cluster has been extensively discussed in the literature [14–17]. Briefly, the $[H_2As_6V_{15}O_{42}(H_2O)]$ cluster consists of 15 distorted VO_5 pyramids and three handle-like As_2O_5 moieties, which encapsulates a water molecule O(3)W at its center. Each As_2O_5 unit is constructed form two AsO_3 triangular units joined together by an oxygen bridge. As shown in Fig. 1, 15 VO_5 pyramids are connected into a cage-like sphere by sharing their basal edges with three "windows" left, which is completed by As_2O_5 moieties by sharing corners.

As shown in Fig. 2, the Co1 atom completes its octahedral configuration by six oxygen atoms from coordinated water molecules, with Co1–O1W 2.195(5) Å and Co1–O2W 2.196(5) Å, respectively. The detailed analysis shows that there are hydrogen bonds between coordinated waters and terminal oxygen atoms (from arsenic–vanadium cluster). The distances of hydrogen bonds through O1W···O5 and O1W···O2 are 3.1187(49) and 3.1086(62) Å, respectively. Interestingly, in the crystal structure, one $[H_2As_6V_{15}O_{42}(H_2O)]^{4-}$ cluster anion directly interacts to its two adjacent neighboring $[H_2As_6V_{15}O_{42}(H_2O)]^{4-}$ cluster anions using three O5 terminal oxygen atoms leading to a perfect equilateral triangle motif (Fig. 2). In the linking region, any two of the three O···O interactions is characterized by the O/O separation of 3.1062(40) Å, which is in the range of hydrogen bonding distance. Examination of the hydrogen bonds of **1** shows that O1W···O5 plays a key role to connect the two adjacent cobalt octahedra into a secondary building unit

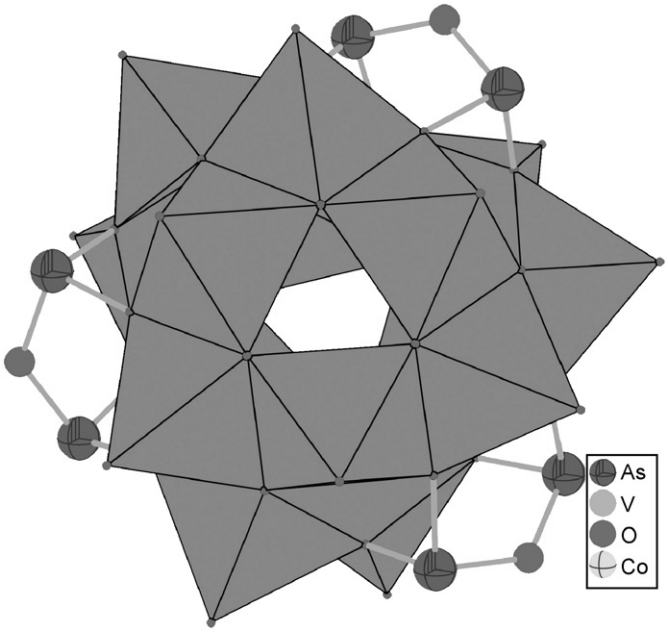

Fig. 1. The polyhedral representation of the $[H_2As_6V_{15}O_{42}(H_2O)]$ cluster.

(SBU) [23], the Co–Co distances is 8.2728(24) Å. Alternatively, two cobalt octahedra are joint together by a triplet formed from three O5 through hydrogen bonding interactions. If the cobalt atoms were neglected, a beautiful oxygen "cluster" would be found which is similar with the traditional water cluster, as shown in Fig. 2.

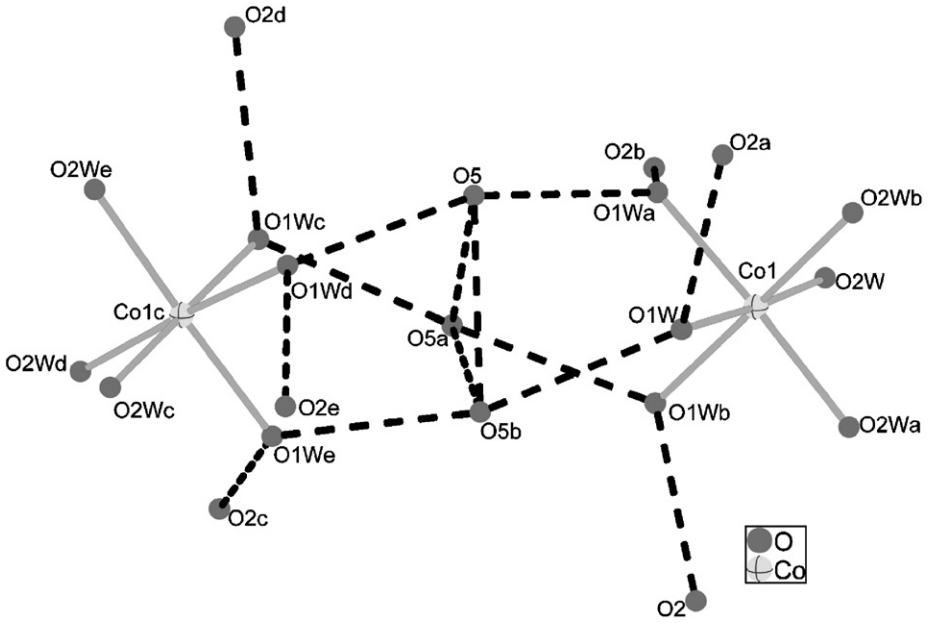

Fig. 2. Drawing of hydrogen bonds of **1**. Hydrogen bonds are indicated by dashed lines: (a) $-y, x-y, z$; (b) $-x+y, -x, z$; (c) $-y, -x, 0.5-z$; (d) $-x+y, y, 0.5-z$ and (e) $x, x+y, 0.5-z$.

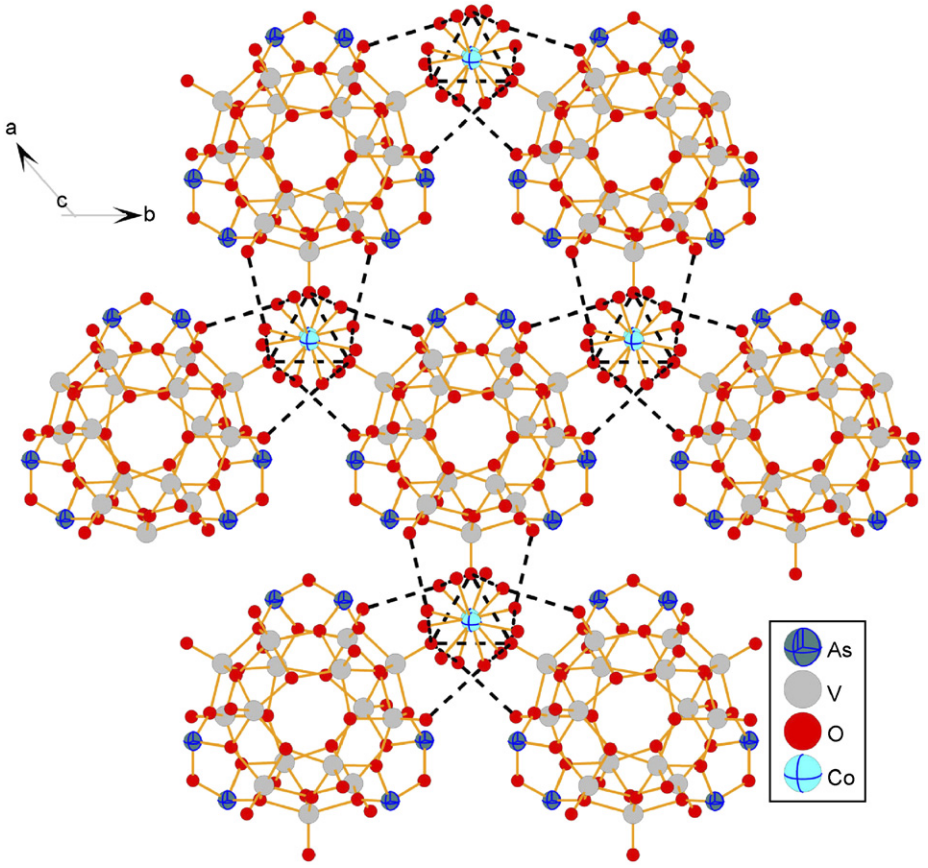

Fig. 3. The representation of the 2-D hydrogen-bonding layer linked by clusters and SBUs.

The most unusual feature of compound **1** is that it presents a novel 2-D supramolecular structure constructed from arsenic–vanadium clusters and the SBUs, as shown in Fig. 3. From upper view, the SBU exhibits a beautiful paddle–wheel motif, each of which acts as a special hexa-dentate ligand supporting three clusters. Alternatively, each cluster interacts with its adjacent six ones by three SBUs through hydrogen bonds. It is worth noting that the equilateral triangle made from three O5 plays a special role in the supramolecular arrangement, which not only comes from clusters as terminal oxygen atoms but also belong to the SBUs, that is, the SBUs share three O5 with three clusters. If there were no cobalt octohedra in the structure, the clusters would interact with one another into a 2-D layer only through interactions occurred among three O5 terminal oxygen atoms. Thereby, the synergistic interactions increase the stability of the structure of compound **1**.

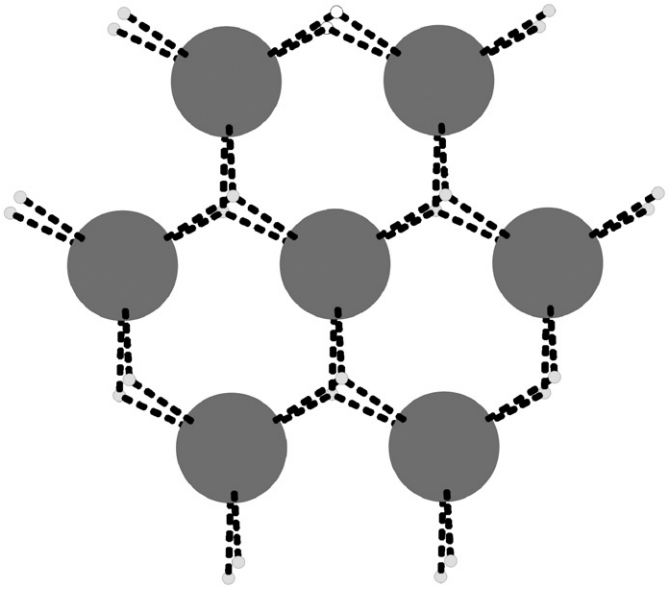

Fig. 4. The topology-view of the layer of the compound **1**, the big circle represents the cluster, and the two small circles represent the SBU, the dashed line represents the hydrogen bond.

It is very interesting to observe the array of the compound **1**, a topology-view of the array is shown in Fig. 4, and it presents a beautiful honeycomb structure. Each honeycomb "cell" consists of three clusters and three SBUs, which are connected alternately. The "cell" is further linked into a 2-D layer by sharing "edges". The centroid–centroid distance of the clusters is 12.5402(18) Å, while the distance of the SBUs is 12.5402(18) Å too.

3.3. ESR, XPS and IR spectra of compounds *1* and *2*

The ESR spectrum of **1** is shown in Fig. 5(a), the curve with $g = 2.06281$ is ascribed to Co^{2+}, and Fig. 5(b) exhibits ESR spectrum of **2** with $g = 2.08279$ attributed to Ni^{2+}. Lack of signals for V^{4+} indicates that the electrons of the cluster are spin–spin coupled. Fig. 6(a) shows the XPS [24] spectrum of **1** in V 2*p* region with peak at 515.9 eV ascribed to V^{4+}, while compound **2** exhibits a similar XPS curve in V 2*p* region with peak at 515.9 eV ascribed to V^{4+} too, shown in Fig. 6(c). Fig. 6(b) shows the spectrum of **1** in Co 2*p* region with peak at 781 eV attributed to Co^{2+}, and in Fig. 6(d), the XPS curve with peak at 855 eV is owed to the Ni^{2+} of compound **2**. The XPS estimation of the valence-state values seems to be in reasonable agreement with those calculated from the bond valence sum calculations [25]. These results further confirm the valences of the arsenic and vanadium atoms.

The infrared spectra of **1** and **2** have been recorded between 4000 and 200 cm^{-1}, both of which exhibit very similar peaks. Strong peaks (985, 727 cm^{-1}) for compound **1** and ones (989, 727 cm^{-1}) for compound **2** are associated with ν_{sym} (V═O) and ν_{asym} (V═O). Similar peaks were also observed in the 463–632 cm^{-1} region for compound **1** (630, 463 cm^{-1}) and compound **2** (632, 463 cm^{-1}) attributed to ν (V–O–V). And a broad band at about 3437 cm^{-1} and a broad band at about 3343 cm^{-1} are associated with the waters of crystallization for compounds **1** and **2**, respectively.

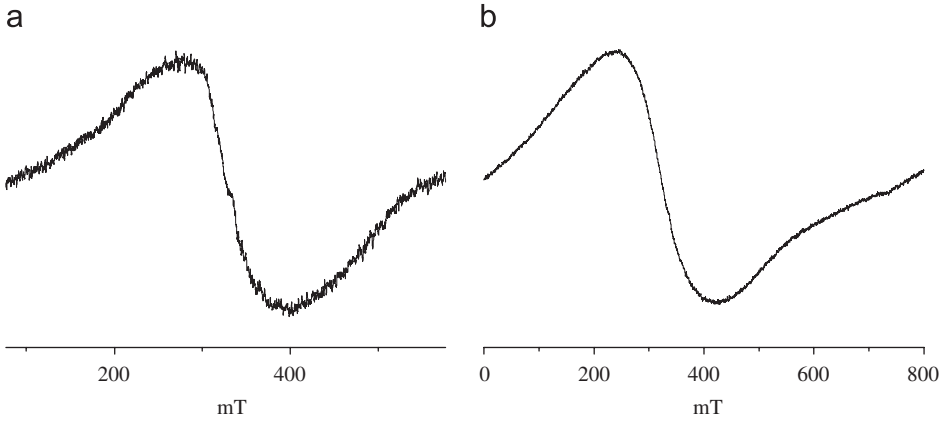

Fig. 5. The ESR spectrum of (a) **1** and (b) **2**.

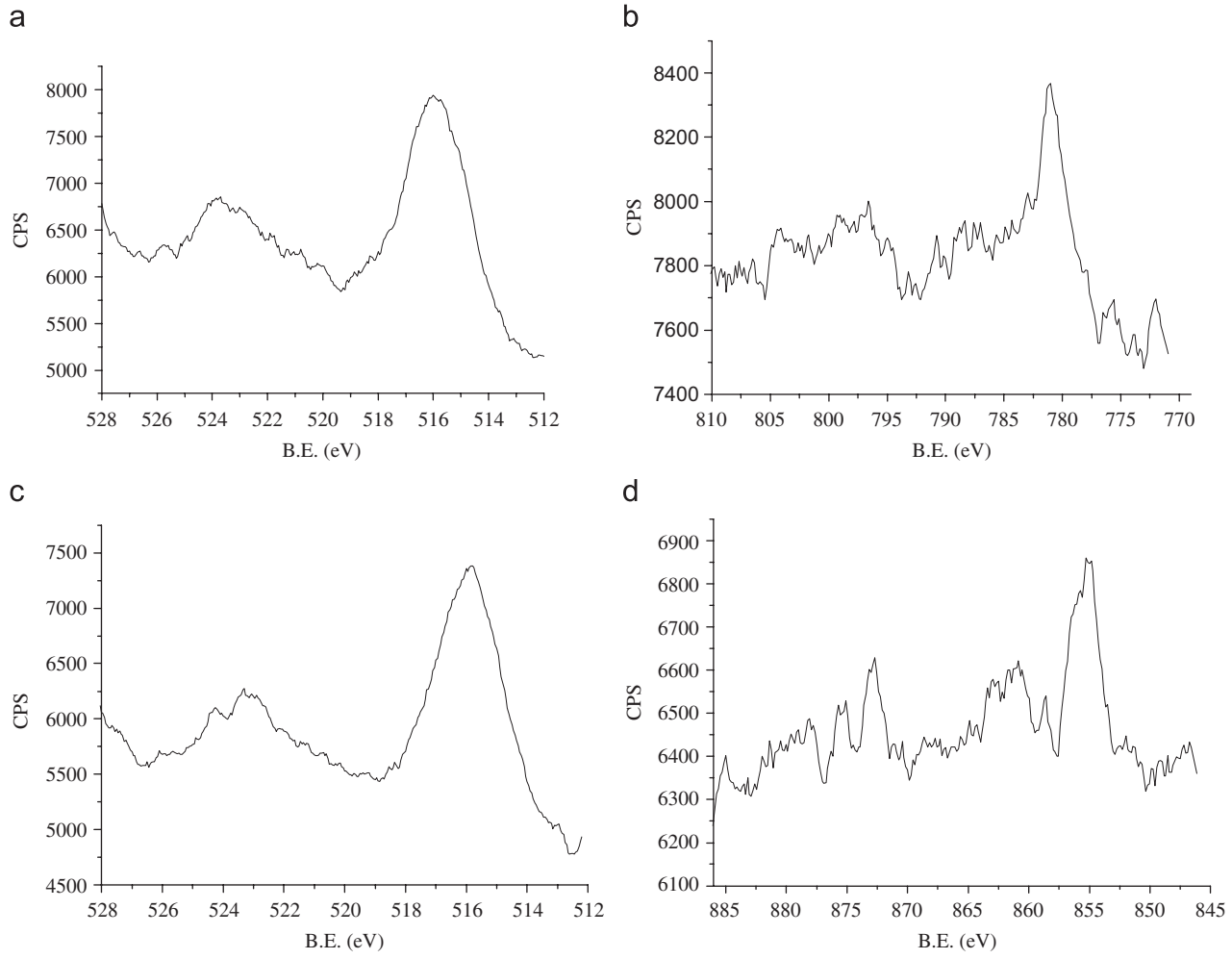

Fig. 6. (a) XPS spectrum of V^{4+} of **1**, (b) XPS spectrum of Co^{2+} of **1**, (c) XPS spectrum of V^{4+} of **2** and (d) XPS spectrum of Ni^{2+} of **2**.

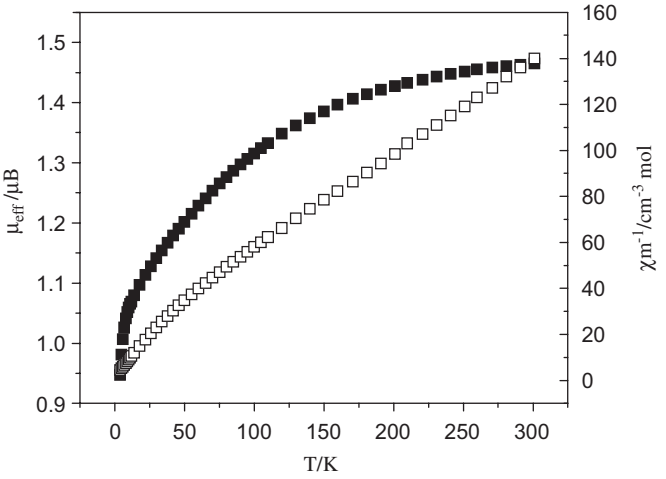

Fig. 7. Temperature dependences of χ_M^{-1} and μ_{eff} for complex **1**.

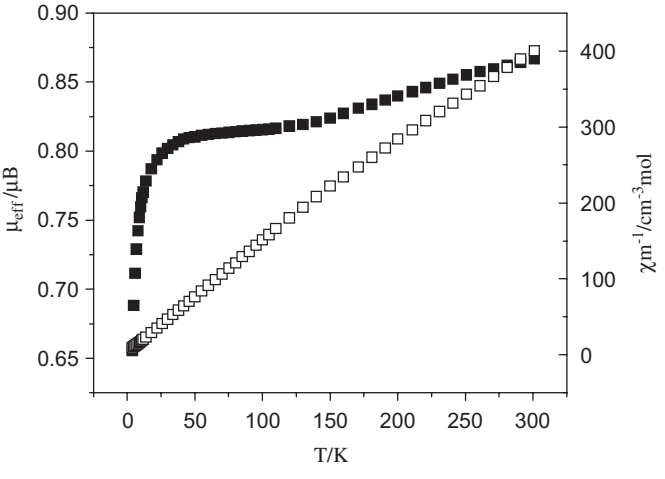

Fig. 8. Temperature dependences of χ_M^{-1} and μ_{eff} for complex **2**.

3.4. Magnetic properties of compounds *1* and *2*

Preliminary magnetic studies have been performed on powdered samples of **1** and **2** in the range of 4–300 K. The temperature dependence of the magnetization was studied in a 1000 Oe field. Fig. 7 shows the magnetic behavior of **1** in the form of μ_{eff} versus T and χ_M^{-1} versus T plots. Upon cooling, the μ_{eff} continuously decreases, indicating the presence of the antiferromagnetic exchange interactions. The magnetic data of sample **1** obeys the Curie–Weiss

law in the range 50–300 K temperature region, and gives values $C = 2.43\ \text{emu mol}^{-1}\ \text{K}$ and $\theta = -38.81\ \text{K}$, characteristic of the antiferromagnetic interactions of **1**. The magnetic behavior of **2** is similar to compound **1**, which is shown in Fig. 8 in the form of μ_{eff} versus T and χ_{M}^{-1} versus T plots. The continuous decrease of the μ_{eff} upon cooling indicates the presence of the antiferromagnetic exchange interactions. The magnetic data of sample **2** obeys the Curie–Weiss law in the range 100–300 K temperature region, and gives values $C = 0.81\ \text{emu mol}^{-1}\ \text{K}$ and $\theta = -27.39\ \text{K}$, characteristic of the antiferromagnetic interactions of **2**. Unfortunately, it is not easy to fit the experimental magnetic data of these two hetero-polymetallic spin systems using suitable theoretical models [26].

4. Conclusions

In conclusion, two new hydrogen-bonded high-dimensional supramolecular architectures have been synthesized and structurally characterized. In these two compounds, supramolecular interactions among the cations and inorganic polyanions play significant roles in stabilization of the overall high-dimensional supramolecular network. Extended researches are underway to reveal the synthetic rules and explore their attractive properties.

Acknowledgment

This work was supported by the National Natural Science Foundation of China (Nos. 20571032 and 20333070).

Appendix A. Supplementary materials

Supplementary data associated with this article can be found in the online version at doi:10.1016/j.jssc.2007.11.020.

References

[1] J.M. Lehn, Supramolecular Chemistry, VCH, New York, 1995.
[2] F. Vögtle, Supramolecular Chemistry, Wiley, Chichester, 1991.
[3] J.-M. Lehn, Comprehensive Supramolecular Chemistry, Pergamon, New York, 1996.
[4] J.M. Lehn, Angew. Chem., Int. Ed. Engl. 29 (1990) 1304.
[5] J.M. Lehn, Supramolecular Chemistry, VCH, Weinheim, 1995.
[6] C.N.R. Rao, S. Natarajan, R. Vaidhyanathan, Angew. Chem., Int. Ed. 43 (2004) 1466.
[7] O.M. Yaghi, M. O'Keeffe, N.W. Ockwig, H.K. Chae, M. Eddaoudi, J. Kim, Nature 423 (2003) 705.
[8] B.F. Abrahams, A. Hawley, M.G. Haywood, T.A. Hudson, R. Robson, D.A. Slizys, J. Am. Chem. Soc. 126 (2004) 2894.
[9] J.L.C. Rowsell, O.M. Yaghi, Microporous. Mesoporous. Mater. 73 (2004) 3.
[10] S.V. Kolotuchin, E.E. Fenlon, S.R. Wilson, C.J. Loweth, S.C. Zimmerman, Angew. Chem. Int. Ed. 34 (1995) 2654.
[11] C. Streb, D.-L. Long, L. Cronin, Cryst. Eng. Commun. 8 (2006) 629.
[12] V. Coué, R. Dessapt, M. Bujoli-Doeuff, M. Evain, S. Jobic, Inorg. Chem. 46 (2007) 2824.
[13] H. Kumagai, M. Arishima, S. Kitagawa, K. Ymada, S. Kawata, S. Kaizaki, Inorg. Chem. 41 (2002) 1989.
[14] A. Müller, J. Döring, Anorg. Allg. Chem. 595 (1991) 251.
[15] G. Huan, M.A. Greaney, A.J. Jacobson, J. Chem. Soc., Chem. Commun. (1991) 260.
[16] A. Müller, J. Döring, Angew. Chem. Int. Ed. Engl. 27 (1988) 1721.
[17] G.-Y. Yang, L.-S. Chen, J.-Q. Xu, Y. Li, H. Sun, Z. Pei, Q. Su, Y. Lin, Y. Xing, Acta Cryst., Sect. C 54 (1998) 1556–1558.
[18] X.-B. Cui, J.-Q. Xu, H. Meng, S.-T. Zheng, G.-Y. Yang, Inorg. Chem. 43 (2004) 8005.
[19] X.-B. Cui, J.-Q. Xu, Y. Li, Y.-H. Sun, G.-Y. Yang, Eur. J. Inorg. Chem. 5 (2004) 1051.
[20] S. Feng, R. Xu, Acc. Chem. Res. 34 (2001) 239.
[21] A. Stein, S.W. Keller, T.E. Mallouk, Science 289 (1993) 1558.
[22] P.J. Hagrman, D. Hagrman, J. Zubieta, Angew. Chem. Int. Ed. Engl. 38 (1999) 2638.
[23] N.L. Rosi, J. Kim, M. Eddaoudi, B. Chen, M. O'Keeffe, O.M. Yaghi, J. Am. Chem. Soc. 127 (2005) 1504.
[24] C.D. Wagner, W.M. Riggs, L.E. Davis, J.F. Moulder, G.E. Muilenberg, Handbook of X-ray Photoelectron Spectroscopy, Perkin-Elmer Corp., MI, 1978.
[25] D. Altermatt, I.D. Brown, Acta Crystallogr., Sect. B 41 (1985) 240.
[26] O. Khan, Molecular Magnetism, VCH, Weinheim, Germany, 1993.